Nature and Surface Redox Properties of Copper(II)-Promoted Cerium(IV) Oxide CO-Oxidation Catalysts

Philip G. Harrison,*[,†] Ian K. Ball,[†] Wan Azelee,[†,‡] Wayne Daniell,[†,§] and Daniella Goldfarb[||]

School of Chemistry, University of Nottingham, University Park, Nottingham NG7 2RD, U.K., and Department of Chemical Physics, The Weizmann Institute of Science, Rehovot, Israel

Received June 29, 2000. Revised Manuscript Received September 19, 2000

$Cu(II)/CeO_2$ catalyst materials have been prepared by two routes, coprecipitation from aqueous solutions containing Cu^{2+} and Ce^{4+} ions and sorption of Cu^{2+} ions on to ceria gel, and their constitutions after thermal treatment in the temperature range 333−1273 K investigated by nitrogen adsorption, powder X-ray diffraction, EPR, and EXAFS. EXAFS data show that the initial Cu(II) species are polymeric $Cu(OH)_2$ and hexaaqua $\{Cu(H_2O)_6\}^{2+}$ ions sorbed onto the surface of the ceria particles from the coprecipitation or impregnation routes, respectively. The materials are mesoporous except after calcination at 1273 K when they become nonporous and crystallites of CuO are apparent. Promotion of ceria with copper(II) enhances the activity toward the oxidation of carbon monoxide dramatically, 100% conversion occurring at 343 K even for high CO concentrations and stoichiometric CO/O_2 compositions. The most active catalyst material is formed by thermal processing of materials obtained by either route at ca. 673 K producing a material comprising small particles of ceria on the surface of which copper(II) is dispersed amorphously. EPR shows that, after calcination at 573 K, the copper(II) is present in both types of material as a mixture of isolated Cu^{2+} ions and amorphous clusters or aggregates of Cu^{2+} ions. Additionally Cu^{2+} dimers are formed at 873 K. In situ redox studies show that the amorphous copper(II) aggregates are reduced most easily by exposure to CO at 473 K, followed by the dimer species at 573 K and finally the isolated Cu^{2+} monomers at 673 K when signals due to Ce^{3+} appear (i.e. reduction of the support). Reoxidation of all types of Cu^+ can be achieved by exposure of the reduced catalyst material to either O_2 or NO, although under the same pressure (200 Torr) oxidation by NO is achieved at a lower temperature than with O_2. The mode of action of these catalyst materials appears to be synergistic in nature with the principal role of Cu(II) being mainly in electron transfer, abstracting the negative charge remaining when oxygen vacancies are formed following desorption of CO_2. The significant enhancement of catalytic activity is due in large part to the efficiency of the Cu(II)/Cu(I) couple in this process. Catalyst deactivation at low temperatures under reducing conditions is due to depletion of the catalyst surface of active oxygen, but activity is restored by treatment in air at moderate temperatures. Deactivation at high temperatures is irreversible and is due to the phase separation of copper(II) oxide coupled with a dramatic increase in particle size.

Introduction

That the promotion of tin(IV) oxide by copper(II) ions has a dramatic effect on its ability to catalyze the oxidation of carbon monoxide using either dioxygen or nitric oxide has been known for some time.[1−3] More recently, however, we have shown that copper(II) has a similar promoting effect on ceria.[4] The nature of these catalyst materials and the role which copper plays in the catalytic processes are subjects of great interest. In general, such catalysts may be prepared by two methods: (i) coprecipitation of a mixed oxide gel from an aqueous solution containing both copper(II) and metal(IV) ions; (ii) sorption of copper(II) ions from aqueous solution onto preformed metal(IV) oxide gel. The principal difference in these procedures is that in the latter the copper should be distributed only on the surface of the metal(IV) oxide particles, whereas in the former some incorporation into the bulk of the oxide may occur.

We have previously[3] investigated the constitution of $Cu(II)/SnO_2$ catalyst materials with Cu:Sn ratios in the range 0.02−0.30 after thermal treatment in the tem-

* To whom correspondence should be addressed.
† University of Nottingham.
‡ Present address: Department of Chemistry, Faculty of Science, University Technology Malaysia, Skudai, Locked Beg 791, 80990 Johor Bahru, Malaysia.
§ Present address: Institut fuer Physikalische Chemie, Ludwig Maximilians Universitaet Muenchen, Butenandtstr. 5-13, 81377 Muenchen, Germany.
|| The Weizmann Institute of Science.

(1) Fuller, M. J.; Warwick, M. E. *J. Catal.* **1974**, *34*, 445.
(2) Fuller, M. J.; Warwick, M. E. *J. Catal.* **1976**, *42*, 418.
(3) Harrison, P. G.; Bailey, Craig; Daniell, D.; Zhao, D.; Ball, I. K.; Goldfarb, D.; Lloyd, N. C.; Azelee, W. *Chem. Mater.* **1999**, *11*, 3643.
(4) Harrison, P. G.; Azelee, W. Pat. appl.

10.1021/cm001113k CCC: $19.00
Published on Web 11/23/2000

perature range 333−1273 K. Materials obtained by coprecipitation or impregnation are similar in nature irrespective of the Cu:Sn ratio. The material formed initially via either route comprises hexaaqua $\{Cu(H_2O)_6\}^{2+}$ ions sorbed onto the surface of the tin(IV) oxide particles <5 nm in size. Thermal processing results in the formation of dispersed amorphous CuO, while calcination at temperatures of ≥873 K causes phase separation of CuO. The particle size does not increase significantly even after calcination at 673 K, but calcination at 873 K results in larger particles. At temperatures ≥1073 K sintering to give very large particles occurs.

In the case of $Cu(II)/SnO_2$ catalysts, we have shown that only surface copper(II) is readily reduced on exposure to carbon monoxide and therefore available for the catalysis process, while copper(II) ions located in the bulk are relatively inert. The mode of operation of the catalysts appears to be synergistic in nature with the principal role of Cu(II) being mainly in electron transfer; i.e., it abstracts the negative surface charges (formed in the oxygen vacancies following desorption of CO_2) to form Cu(I), which is then oxidized back to Cu(II) by reaction with oxygen. The activity of catalysts deactivated by running under highly reducing conditions can be restored completely by heating in a flow of air at 355 K. Irreversible deactivation occurs on processing at very high temperatures due to sintering and the phase separation of copper(II) oxide.

Here we present details of the nature and activity toward the catalytic oxidation of carbon monoxide of $Cu(II)/CeO_2$ catalysts prepared by similar impregnation and coprecipitation methods in order to compare their behavior on thermal processing with the analogous $Cu(II)/SnO_2$ materials. Further, EPR has been used to study the role of the paramagnetic copper(II) centers and the surface redox properties of these catalytic materials.

Experimental Section

Catalyst Preparation. *Cerium(IV) Oxide.* Ceria was prepared by the ammonia precipitation method from an aqueous solution of cerium(III) nitrate hexahydrate. To this vigorously stirred solution was added a mixture of aqueous ammonia and hydrogen peroxide (10:1) dropwise over a period of 1 h until the solution reached pH 10. After the solution was stirred overnight at ambient temperature the resulting yellow-brown precipitate was washed in triply distilled water and centrifuged three times. The solid was air-dried overnight at 383 K giving a pale yellow gel.

Copper(II)-Promoted Cerium(IV) Oxide. (a) By Impregnation. A slurry of ceria powder (5 g) in a solution of copper(II) nitrate trihydrate in triply distilled water (50 mL) was stirred vigorously at ambient temperature. The concentration of the solution was adjusted according to the desired Cu:Ce atom ratio. The resulting suspension was then filtered and dried overnight in air at 333 K. At no time was the solid washed in order to prevent any loss of loosely bound copper. Samples were pale green (higher Cu content) to pale yellow (low Cu content) in color. These samples are designated Cu/CeO_2-imp with the Cu:Ce atom ratio denoted in parentheses.

(b) By Coprecipitation. Samples were prepared by the coprecipitation method from a solution containing both copper(II) nitrate trihydrate and cerium(III) nitrate hexahydrate in triply distilled water. All samples were dark green in color independent of the copper content. These samples are designated Cu/CeO_2-cop with the Cu:Ce atom ratio denoted in parentheses.

Catalyst Thermal Pretreatment. Copper(II)-promoted ceria catalyst materials (approximately 2 g aliquots) were calcined in an alumina boat for 24 h using a Vecstar 91e tube furnace at temperatures in the range 573−1273 K. Samples developed a pink coloration at high temperatures.

Physical and Spectroscopic Measurements. Gas adsorption data were obtained using a Micromeretics instrument. XRF data were kindly obtained by LSM Ltd., Rotherham, U.K., using a Philips PW1480 wavelength dispersive instrument. Samples were prepared as a 10% dilution in a lithium tetraborate bead. Infrared spectra were obtained from KBr disk samples using a Nicolet 20SXC spectrometer. A total of 32 scans were recorded for each sample at a resolution of 1 cm^{-1}. EPR measurements were recorded at room temperature using a Bruker EMX EPR spectrometer equipped with a Bruker ER 041 XG microwave bridge in X-band at ca. 9.2 GHz. Experimental g values were determined with reference to diphenylpicrylhydrazyl (DPPH) ($g = 2.0036$).

Powder X-ray diffraction data was acquired using a Philips X-pert system fitted with a PW 1710 diffractometer control unit with Cu Kα radiation ($\lambda = 1.5405$ Å). Representative diffractograms were acquired over 5−80° in 2θ with 0.02° steps and 0.4 s acquisition times per step. DICVOL91[5] was used for indexing. Phase identification was corroborated by comparison to the JCPDS database[6]

EXAFS measurements were performed on station 8.1 at the Daresbury Laboratory, Warrington, U.K, which operates at an energy of up to 2.0 GeV and a maximum beam current of 200 mA. The X-rays are vertically collimated producing a beam of less than 1 mrad divergence. A Si(111) double crystal monochromator was used to select a single-wavelength beam of X-rays, the tuneable energy range that can be achieved using this monochromator is 2−10 keV. A 40−50% amount of the X-ray beam was rejected to filter out the undesired harmonics while retaining 50−60% of the primary beam intensity.

Data were collected at the Cu K-edge (8978.9 keV) in fluorescence mode utilizing a Ge-13 channel solid-state detector. The sample was positioned at ca. 45° to the incident beam so as to maximize the solid angle seen by the detector which was orthogonal to the beam. A total of 6 scans were recorded for each catalyst sample, and refinement was achieved using EXBACK, EXCALIB, and EXCURV92.[7] The scans were coaligned, spikes due to noise removed, and the total number of scans added together to produce a single output data set with an improved signal-to-noise using EXCALIB. Background X-ray absorption was removed from the summed data set in two stages using the program EXBACK. Initially the preedge background was determined by fitting this region to a polynomial usually of order 1. The background absorption was then removed from the postedge region by a series of linked polynomial curves (normally 2 or 3) of order 3. With both the preedge and postedge background absorption removed from the data, the x-axis was converted from energy to k-space ($k = 2\pi/\lambda$, where λ is the electron wavelength) to give the EXAFS oscillations form $k = 0$. The EXAFS were then multiplied to k^3 so as to increase the amplitude of the oscillations at high values of k. Finally, radial distribution spectra were obtained via Fourier transformation of the EXAFS data. EXCURV92 was used to simulate EXAFS spectra of radial shells of neighbors around the central atom. For a more detailed description of the curved wave theory used in the program to calculate theoretical backscattering amplitudes and phase shifts the reader is directed to the publications of Gurman[8] and Lee.[9]

(5) DICVOL91; Boultif, A.; Louer, D. *J. Appl. Crystallogr.* **1991**, *24*, 987.

(6) *JCPDS International Centre for Diffraction Data: Powder Diffraction File: Inorganic Phases*; American Society of Material Testing: West Conshohocken, PA, 1991.

(7) EXBACK, EXCALIB, and EXCURV92, Daresbury Computer programs, Daresbury Laboratory, Cheshire, U.K.

(8) Gurman, S. J.; Binstedt, N.; Ross, I. *J. Phys. C* **1984**, *17*, 143; **1986**, *19*, 1845.

(9) Lee, P. A.; Pendry, J. B. *Phys. Rev. B* **1975**, *11*, 2795.

Table 1. Analytical Data for Cu/CeO₂ Catalyst Materials

sample	Cu:Ce target ratio	Cu content/wt %	Cr content/wt %	actual Cu:Ce ratio
Cu/CeO₂-cop (0.04)	0.11	3.58	86.18	0.04
Cu/CeO₂-cop (0.07)	0.25	5.88	80.46	0.07
Cu/CeO₂-cop (0.09)	0.43	7.12	76.40	0.09
Cu/CeO₂-imp (0.03)	0.11	3.12	89.44	0.03
Cu/CeO₂-imp (0.06)	0.25	5.52	85.07	0.06

The fit correlation parameter R between the calculated and observed data fall in the very acceptable range 20−40. Values of $R < 50$ are not unreasonable for this type of sample, and values of $R < 20$ are unobtainable except for crystalline structures of clearly defined geometries. The estimated levels of accuracy in the refinements made by the EXCURV92 program arising from imperfect transferability of phase shifts and the fitting procedures are the following: coordination number (50%); Debye−Waller factor, $2\sigma^2$ (50%); radii (0.03 Å). The significance of extra shells was evaluated using the reduced χ^2 test, $N_p = [\{(2.\Delta k \Delta R)/\pi\} + 1]$, where N_p is the maximum number of variables and Δk and ΔR are the ranges in k- and r-space, respectively.

EPR Measurements. Reactions were carried out in situ using a modified EPR tube with connections to a vacuum line. Gas flow to and from the cell was controlled by a two tap system connected to the cell by metal screw thread fittings. Gas was passed throught the sample using a perforated glass capillary inserted into the powdered sample, ensuring maximum contact between gas and sample. The sample was heated by inserting the tube into a sleeve of heating tape, allowing a maximum temperature of 673 K to be achieved.

Samples were initially exposed to a reducing atmosphere of carbon monoxide and heated for a set length of time. The state of sample reduction was then monitored by recording the EPR spectrum. The pressure of CO was increased until the sample showed signs of reduction indicated by a decrease in intensity of the Cu(II) resonance. The gas pressure and temperature were subsequently increased until reduction was complete. After evacuation of the sample tube, samples were reoxidized by heating in an oxygen or nitric oxide atmosphere.

Catalysis Measurements. Catalytic conversion data for the oxidation of carbon monoxide were obtained using a custom built horizontal geometry continuous-flow microreactor. The furnace consisted of a stainless steel tube surrounded by a cylindrical stainless steel heating block. The sample tube, which sits inside the stainless steel tube, is made of Pyrex glass 1 cm in diameter with a glass sinter in the middle. The catalyst sample (0.5 g) was packed on the inlet side of the sinter, supported by dry silica gel pellets, and held in place with glass wool. The outlet side of the sinter was packed with dry silica gel pellets also held in place with glass wool. Catalyst samples were sieved to a particle size range of 38−63 μm and diluted with silica gel of particle size 100 μm. Catalyst samples were activated by preheating in situ in the microreactor at 573 K for 2 h under a flow of air and then allowed to cool also under a flow of air. Catalyst temperatures were measured using a thermocouple located as close to the catalyst as possible. Gas flows were controlled by mass flow controllers (Brooks 5850TR), and concentrations of gas-phase components were measured using precise integration of characteristic infrared peak envelopes (CO 2240−2024 cm^{-1}, CO_2 2380−2259 cm^{-1}, NO 1944−1804 cm^{-1}, NO_2 1645−1576 cm^{-1}, and N_2O 2254−2220 cm^{-1}).

Results

Preparative Methodology. The observations reported here indicate that both impregnation and coprecipitation are poor methods for the preparation of copper(II)-promoted ceria materials. Although the copper content in the final samples does increase with increasing concentration of the copper(II) nitrate solution employed, the actual Cu:Ce atom ratios in the resulting materials are far lower than their intended values (in both systems only averaging 25% of target ratios) (Table 1). In the coprecipitation procedure this is probably due to the formation of $[Cu(OH)_4^{2-}]$ and $[Cu(NH_3)_4^{2-}]$ ions due to the high pH (10−12) and high ammonia concentration used. The low loadings achieved during the impregnation method could be improved by adsorption at a pH close to the isoelectronic point rather than under the neutral conditions employed here. Nevertheless, copper(II) loadings in the range 4−9 at. % were achieved as homogeneous materials.

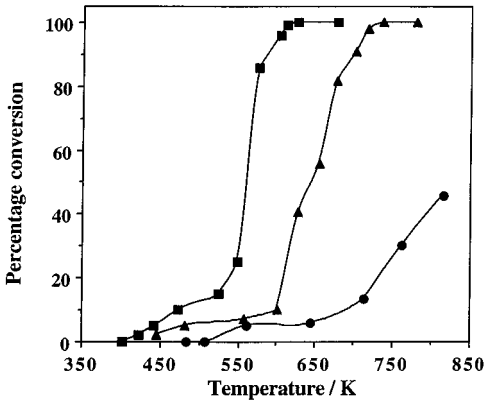

Figure 1. Percentage conversion versus temperature plots for the oxidation of CO over CeO_2 precalcined at 673 K (■), 873 K (▲), and 1273 K (●).

Table 2. Effect of Copper Loading and ex Situ Calcination Temperature on the Catalytic Activity of Cu(II)-Promoted Ceria Materials toward CO Oxidation

Cu:Ce atom ratio	calcination temp/K	light-off temp/K	T_{100} (CO) temp/K
0.04	383	308	378
0.07	383	308	353
	673	323	343 (328[a])
	873	348	358
	1273	493	553
	673[b]	358	368
0.09	383		358

[a] Once activated (see text). [b] No pretreatment.

Catalytic Oxidation of Carbon Monoxide over Copper(II)-promoted Ceria. *(a) Using Dioxygen.* Unpromoted cerium(IV) oxide itself exhibits reasonable activity toward the oxidation of CO under oxygen-rich conditions (5% CO, 20% O_2, 75% N_2), with 100% conversion being achieved in all cases with the exception of the 1273 K calcined material (Figure 1), which gave only 45% conversion at 773 K. Copper(II)-promoted ceria catalysts are, however, significantly more active. Although activity was related to the loading of copper and the temperature of thermal pretreatment, it appeared to be essentially independent of preparative route. Hence, for the purposes of catalytic activity testing, only coprecipitated material was examined. All conversions was carried out using a stoichiometric gas mixture (30% CO, 15% O_2, 55% N_2). Data are listed in Table 2. Specific activity of the ceria-based materials was typically

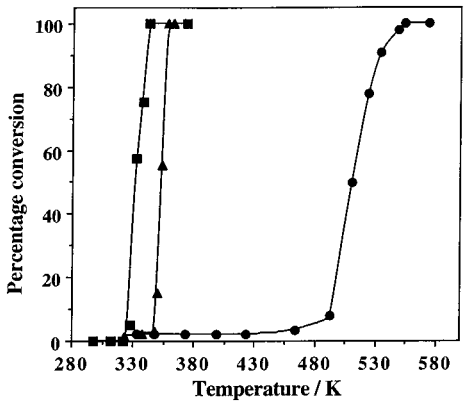

Figure 2. Percentage conversion versus temperature plots for the oxidation of CO over Cu(II)/CeO_2-cop at Cu:Ce loadings of 0.09 (■), 0.07 (▲), and 0.04 (●).

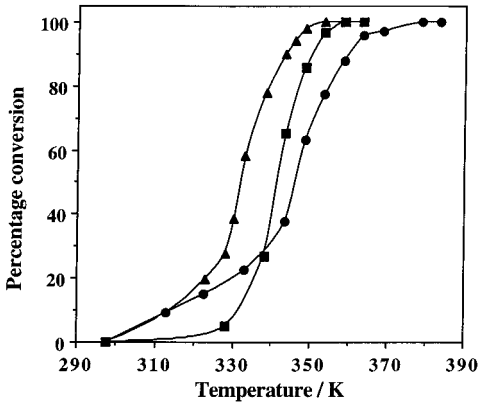

Figure 3. Percentage conversion versus temperature plots for the oxidation of CO over Cu(II)/CeO_2-cop (Cu:Ce = 0.07) precalcined at 673 K (■), 873 (▲), and 1273 (●).

around 0.161(3) mol g^{-1} h^{-1} under stoichiometric conditions and 0.027(1) mol g^{-1} h^{-1} for oxygen-rich experiments.

The catalytic activity of the Cu(II)/CeO_2 catalyst materials does not appear to be greatly influenced by the loading of copper, though activity seems to reach an optimum level with 6 wt % copper (Cu:Ce = 0.07) content. Conversion plots for three catalysts with different loadings of copper activated at 573 K are shown in Figure 2.

Increasing ex situ calcination temperature leads to a decrease in the activity of the Cu(II)/CeO_2-cop (Cu:Ce 0.07) catalyst material (Figure 3). Calcination at 673 K gives optimum activity with complete CO conversion under stoichiometric conditions by 343 K. Calcination at 1273 K causes the greatest decrease in activity with complete conversion not occurring until a temperature of 553 K.

The Cu(II)/CeO_2-cop (Cu:Ce 0.07) catalyst material after ex situ calcination at 673 K shows the remarkable ability to fully oxidize CO under stoichiometric conditions by 343 K. Once activated, the reaction is self-sustaining and will maintain 100% conversion for over 24 h. During this time, the system adopts an equilibrium temperature of 338 K due to the exothermic nature of the oxidation reaction occurring on the catalyst surface. When deactivated by flowing neat CO over the sample for 2 h, the catalyst can be reactivated by heating in a flow of air (100 mL min^{-1}) at 348 K for 3 h, after which 100% conversion is once again exhibited.

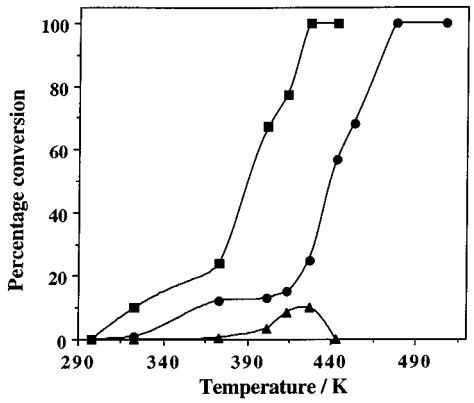

Figure 4. Percentage conversion versus temperature plots for the CO/NO reaction over Cu(II)/CeO_2-cop (Cu:Ce = 0.07) (NO (■), N_2O (▲), and CO (●)).

Table 3. Pore Texture Data for CeO_2 and Cu/CeO_2 Catalyst Materials

sample	calcination temp/K	BET surf area/m^2 g^{-1}	tot. pore vol/ cm^3 g^{-1}	av pore diameter/nm
CeO_2	333	132	0.221	6.7
	673	92	0.193	8.1
	873	43	0.142	12.5
	1073	19	0.090	16.8
	1273	6	0.032	18.9
Cu/CeO_2-cop				
Cu:Ce = 0.04	383	180	0.291	6.4
Cu:Ce = 0.07	383	181	0.250	5.6
	673	106	0.190	7.2
	873	57	0.129	9.1
	1273	0.3	0.002	2.0
Cu:Ce = 0.09	383	182	0.280	6.2
Cu/CeO_2-imp				
Cu:Ce = 0.03	383	120	0.180	6.1

(b) Using Oxides of Nitrogen. Conversion of both CO and NO starts at ca. 325 K when a CO/NO gas mixture (0.5% NO, 5% CO, 94.5% N_2) is passed over the Cu(II)/CeO_2-cop (Cu:Ce 0.09) catalyst precalcined at 673 K for 16 h and activated in situ in air at 573 K for 3 h. In addition small amounts of N_2O are also formed at temperatures of ca. 370−390 K (Figure 4). NO is completely reduced by 428 K with complete oxidation of CO finally occurring at ca. 473 K.

Decomposition of N_2O in the absence of a reductant (1% N_2O, 99% N_2) occurs at 773 K over the same catalyst. The presence of CO (1% N_2O, 5% CO, 95% N_2) lowers the temperature for complete conversion of N_2O to 418 K, though CO itself is not fully oxidized until 588 K.

Pore Texture Data. Pore texture data are collected in Table 3, and a typical isotherm is shown in Figure 5. Isotherms for all the materials studied were of type IV with hysteresis indicative of mesoporous solids, except for materials calcined at 1273 K which were nonporous. The BET surface areas, pore volumes, and average pore diameters for all three Cu(II)/CeO_2-cop materials after drying at 383 K are very similar showing that the level of copper loading has little effect on the pore texture. The BET surface area and pore volume of the Cu(II)/CeO_2-imp (Cu:Ce 0.03), however, are significantly lower although the average pore diameter is similar to the Cu(II)/CeO_2-cop materials, possible indicating some blocking of the pores by adsorbing $[Cu(OH_2)_6^{2+}]$ cations. Increasing the calcination temperature results in a steady decrease in the surface area and total pore

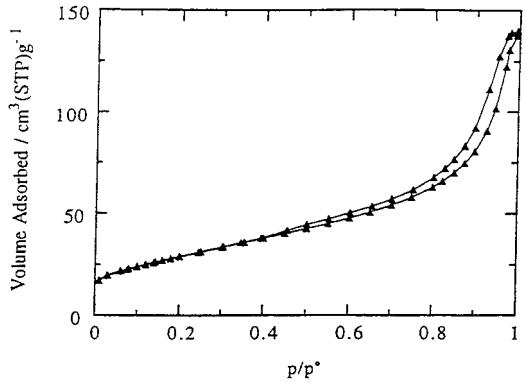

Figure 5. Typical BET isotherm of the Cu(II)/CeO_2-cop (Cu:Ce = 0.06) catalyst material after calcination at 673 K.

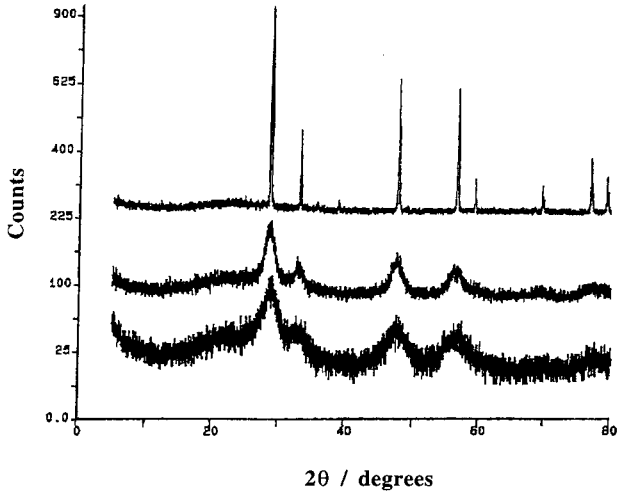

Figure 6. Powder X-ray diffractograms of the Cu(II)/CeO_2-cop (Cu:Ce = 0.06) catalyst material after calcination at temperatures of 383 K (bottom), 573 K (middle), and 1273 K (top).

volume reaching values of 57 $m^2\ g^{-1}$ and 0.129 $cm^3\ g^{-1}$ after calcination at 873 K, while the average pore diameter increases from ca. 6 nm at 383 K to ca. 9 nm at 873 K. At this temperature the particle size of the ceria crystallites has increased by a factor of ×3 and crystallites of CuO are apparent. On further calcination at 1273 K the material undergoes sintering and densification giving large particles of both components which exhibit negligle pore structure. Similar behavior is shown by ceria itself, although in this case the pore diameter increases greatly with increasing calcination temperature.

Powder X-ray Diffraction. Both the Cu(II)/CeO_2-cop and Cu(II)/CeO_2-imp materials exhibited very similar diffractograms at each calcination temperature and only differed in the relative intensity of the CuO phase observed at temperatures above 873 K. For this reason, only the behavior of the Cu(II)/CeO_2-cop (Cu:Ce = 0.06) material is described and diffractograms of this material after thermal treatment in the range 333−1273 K are shown in Figure 6. After being dried at 333 K, the material exhibits broad poorly resolved peaks. However, calcination at 573 K leads to a sharpening of these peaks, which at 873 K are clearly attributable to CeO_2. A series of much weaker bands is also now apparent which become more resolved at 1273 K. The two phases were identified as cubic CeO_2 (a = 5.421 Å, V = 159.30 Å^3; lit.[10] a = 5.411 Å, V = 158.46 Å^3) (major component), and monoclinic CuO (a = 4.631 Å, b = 3.429 Å, c = 5.187 Å, V = 82.36 Å^3); lit.[11] a = 4.684 Å, b = 3.425 Å, c = 5.129 Å, V = 81.16 Å^3) (minor component). Relative peak intensities and d-values indicate that no solid solution formation occurs and that two separate oxide phases are formed at calcination temperatures >873 K. Indexing and calculated unit cell dimensions indicate that no incorporation of copper into the ceria lattice occurs.

Table 4. Refined Structural Parameters from Cu K-Edge EXAFS Data for the Cu(II)/CeO_2-imp (Cu:Ce = 0.06) Catalyst Material after Calcination at Various Temperatures in the Range 333−1273 K[a,b]

calcination temp (K)	atom type	coord no.	radial dist/Å	Cu species present	lit. values/Å
333	O	4	1.959	$[Cu(OH_2)_6^{2+}]$[c]	1.955
	O	2	2.120		2.381
	O	2	3.047		
	O	2	3.344		
573	O	4	1.952	isolated Cu^{2+}	
	O	2	2.133	species	
	O	4	3.544		
873	O	2	1.955	CuO[d]	1.951
	O	2	1.974		1.961
	O	2	2.809		2.784
	Cu	4	2.929		2.901
	Cu	4	3.105		3.083
1273	O	2	1.952	CuO[d]	1.951
	O	2	1.964		1.961
	O	2	2.779		2.784
	Cu	4	2.911		2.901
	Cu	4	3.112		3.083
	Cu	2	3.204		3.173
	O	2	3.494		3.408

[a] R values 32.0 (333 K), 45.0 (573 K), 38.0 (873 K), and 35.0 (1273 K). [b] Average Debye−Waller factors (ranges in parentheses): 0.005 Å^2 (0.001−0.012 Å^2) (333 K), 0.012 Å^2 (0.005−0.021 Å^2) (573 K), 0.007 Å^2 (0.003−0.010 Å^2) (873 K), and 0.013 Å^2 (0.001−0.025 Å^2) (1273 K). [c] Reference 12. [d] Reference 13.

Average crystallite sizes calculated using the Scherrer equation were for the CeO_2 phase 2.5, 8.0, and 85.0 nm following calcination at 573, 873, and 1273 K, respectively, and for the CuO phase 3.5 nm at 873 K and 63.5 nm at 1273 K. Average particle sizes of both phases were confirmed by TEM analysis.

Extended X-ray Absorption Fine Structure Spectroscopy. Results of the refinement of the EXAFS data for the Cu(II)/CeO_2-imp (Cu:Ce = 0.06) and Cu(II)/CeO_2-cop (Cu:Ce = 0.07) materials are presented in Tables 4 and 5, respectively.

Copper(II) ions in the Cu(II)/CeO_2-imp (Cu:Ce = 0.06) material dried at 333 K exhibit a typical [4 + 2] Jahn−Teller-distorted coordination by six oxygen atoms. The next-nearest neighbors are four oxygens at 3.05 Å (×2) and 3.34 Å (×2). No other metal atom is present until at least >5 Å. This would suggest that the copper is present as adsorbed isolated Cu(II) ions which are hydrogen-bonded to the (hydroxylated) ceria surface.

A similar coordination geometry is indicated in the refinement of the material calcined at 573 K, with a primary Jahn−Teller-distorted [4 + 2] oxygen six-coordination and a further four oxygen atoms at a distance of ca. 3.5 Å. However, in this case the refinement is considerably improved by the inclusion of a cerium atom at a distance of ca. 4.2 Å, indicating closer

(10) CeO_2: JCPDS File No. 34-394.
(11) CuO: JCPDS File No. 5-661.

Table 5. Refined Structural Parameters from Cu K-Edge EXAFS Data for the Cu(II)/CeO_2-cop (Cu:Ce = 0.07) Catalyst Material after Calcination at Various Temperatures in the Range 333−1273 K[a,b]

calcination temp (K)	atom type	coord no.	radial dist/Å	Cu species present	lit. values/Å
333	O	2	1.950	$Cu(OH)_2$[c]	1.948
	O	2	1.972		1.972
	O	1	2.378		2.356
	O	1	2.898		2.915
	Cu	2	2.960		2.947
	Cu	2	3.328		3.340
573	O	2	1.930	isolated Cu^{2+}	
	O	2	1.979	species	
	O	1	2.520		
	O	1	2.905		
873	O	2	1.956	CuO[d]	1.951
	O	2	1.966		1.961
	O	2	2.739		2.784
	Cu	4	2.955		2.901
	Cu	4	3.121		3.083
1273	O	2	1.955	CuO[d]	1.951
	O	2	1.970		1.961
	O	2	2.759		2.784
	Cu	4	2.892		2.901
	Cu	4	3.051		3.083
	Cu	2	3.161		3.173

[a] *R* values 28.0 (333 K), 49.0 (573 K), 42.0 (873 K), and 38.0 (1273 K). [b] Average Debye−Waller factors (ranges in parentheses): 0.007 Å^2 (0.002−0.015 Å^2) (333 K), 0.011 Å^2 (0.009−0.022 Å^2) (573 K), 0.012 Å^2 (0.008−0.027 Å^2) (873 K), and 0.008 Å^2 (0.002−0.012 Å^2) (1273 K). [c] Reference 14. [d] Reference 13.

proximity of the adsorbed [$Cu(OH_2)_6^{2+}$] cations to the surface of the ceria particles.

Calcination at temperatures of ≥873 K result in dramatic changes in the radial functions, with peaks emerging at distances of ca. 2.9 and 3.3 Å, and the EXAFS data refine well for CuO (Table 4). CuO is just discernible by XRD at 873 K, but it is not until 1273 K that a clear diffractogram is obtained. EXAFS shows quite clearly that CuO clusters have formed by 873 K but are not necessarily crystalline at this temperature.

EXAFS data for the Cu(II)/CeO_2-cop (Cu:Ce = 0.07) material dried at 333 K also indicates a local Jahn−Teller-distorted [4 + 2] oxygen six-coordination at copper (Table 5). However, in this case successive shells appear to be better represented by polymeric copper(II) hydroxide,[14] $Cu(OH)_2$, rather than by adsorbed [$Cu(OH_2)_6^{2+}$] cations. In particular the presence of copper atoms at 2.96 Å (×2) and 3.28 Å (×2) suggests the presence of $Cu(OH)_2$ clusters for the material dried at 333 K. The copper environment after calcination at 573 K is similar, although in this case the copper shells at ca. 3 Å are not apparent indicating the presence of essentially isolated Cu(II) ions. Further, the refinement of these data is significantly improved by the incorporation of a cerium atom at a distance of ca. 4.2 Å, and hence, it would appear that essentially isolated Cu(II) ions are dispersed over the surface of ceria particles bringing the copper into closer proximity to the particle surface. However, it is unreasonable to exclude the possibility of the presence of adsorbed [$Cu(OH_2)_6^{2+}$] cations in both of these samples.

(12) Gallucci, J. C.; Gerkin, R. E. *Acta Crystallogr. C* **1989**, *45*, 1279.
(13) Åsbrink, S.; Lorrby, L. J. *Acta Crystallogr. B* **1970**, *26*, 8.
(14) Oswald, H. R.; Reller, A.; Schmalle, H.; Dubler, E. *Acta Crystallogr. B* **1990**, *46*, 2279.

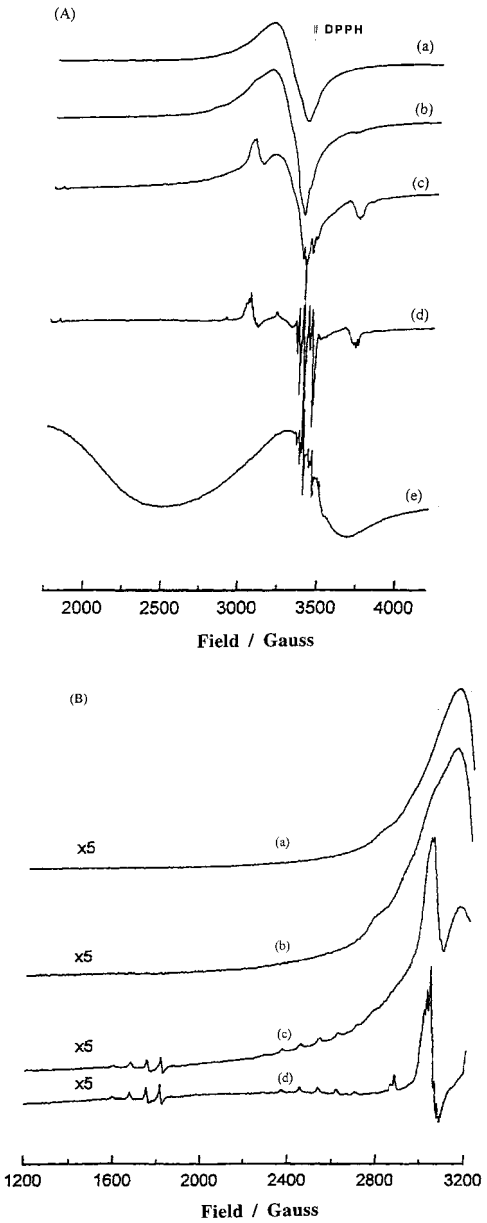

Figure 7. (A) ESR spectra of the Cu(II)/CeO_2-cop (Cu:Ce = 0.06) catalyst material after drying at 333 K (a) and after calcination at 573 K (b), 873 K (c), 1073 K (d), and 1273 K (e). (B) Low-field region (×5) of the same sample.

Data for the Cu(II)/CeO_2-cop (Cu:Ce = 0.07) material after calcination at calcination temperatures of ≥873 K is essentially identical to that of the Cu(II)/CeO_2-imp (Cu:Ce = 0.06) material, with good fits of the data to CuO.

Electron Paramagnetic Resonance Spectroscopy. Figure 7A shows the EPR spectra obtained after calcination of the Cu/CeO_2-cop (Cu:Ce = 0.09) material after calcination at temperatures between 383 and 1273 K. The spectrum changes with increasing calcination temperature from a simple, broad signal (similar to that exhibited by aqueous copper hexaaqua ions) to a complex array of well-resolved narrow lines. Four different copper EPR signals are observed over the calcination range which have the following assignments. The first is a broad isotropic signal ($g_{iso} \approx 2$) observed at low calcination temperatures and is attributed to Cu^{2+} ions in the form of amorphous copper(II) aggregates present

on the surface of the ceria particles (type B signal).[15] The second signal, which has an axial symmetry, is present at all temperatures and becomes more clearly resolved with increasing calcination temperature, adopting parallel and perpendicular components of the hyperfine structure. The EPR parameter values of this signal ($g_{\|} = 2.248$, $g_{\perp} = 2.092$, $A_{\|} = 120$G, $A_{\perp} = 28$G) are characteristic of isolated Cu^{2+} ions located in tetragonally distorted octahedral sites (type A signal).[15] The third copper signal is also isotropic ($g_{iso} = 2.098$), is seen only with high copper concentrations and after calcination at high temperature, and is attributed to CuO particles. The final signal, which appears complex, is observed after calcination at 873 K and becomes more clearly resolved at higher temperatures. This signal has been extensively studied[15,16] and attributed to copper(II) ion dimers (type K signal)[15] and exhibits fine and hyperfine structure ($g_{\|} = 2.195$, $A_{\|} = 85$G; $g_{\perp} = 2.031$, $A_{\perp} = 12$ G) arising from the coupling between unpaired electrons of two Cu^{2+} ions ($I = 3/2$). Each component of the fine structure comprises seven narrow lines with relative intensities 1:2:3:4:3:2:1. Associated with this triplet signal is a weak intensity signal at low magnetic field (ca. 1700 G) which is characteristic of the dimeric species arising from a forbidden transition. Since the hyperfine splitting constants belonging to the isolated Cu^{2+} ions are double those of the dimeric species (and the *g*-values are very similar), it has been suggested that the isolated monomeric Cu^{2+} ions are located in sites on the ceria surface similar to those of the dimers and are in fact their precursors.[15] Figure 7B is an enlarged section of the low magnetic field region which allows a clearer view of this "half-field" signal ($g = 4.133$). These data should be compared with those observed for a Cu(II)/CeO_2-cop (Cu:Ce 0.01) material calcined at 1173 K which exhibited two A type signals with parameters $g_{\|} = 2.2079$, $g_{\perp} = 2.0403$, $A_{\|} = 170$ G, $A_{\perp} = 27$ G (A_1) and $g_{\|} = 2.1233$, $g_{\perp} = 2.0758$, $A_{\|} = 82$ G, $A_{\perp} = 40$ G (A_2) and a type K signal with parameters $g_{\|} = 2.2079$, $g_{\perp} = 2.0403$, $A_{\|} = 85$G, $A_{\perp} = 13.5$ G.[15]

Figure 8 shows the EPR spectra recorded for the Cu/CeO_2-imp (Cu:Ce = 0.06) material calcined over the range 333−1273 K. The EPR spectrum obtained for the sample after drying at 333 K comprises the superposition of two signals. The first, which has poorly resolved hyperfine structure ($g_{\perp} = 2.032$), is characteristic of Cu^{2+} ions with axial symmetry (type C signal). The second broader signal is isotropic and centered at $g_{iso} = 2.142$ (ΔH = ca. 200 G) and can be assigned to aggregates of copper(II) in which the copper(II) ions are in close enough proximity to give rise to dipolar broadening (type B signal). No trace of either Ce^{3+} or the superoxide ion (O_2^-) was detected. Calcination at 873 K leads to the appearance of a triplet signal assigned to copper(II) ion dimers (type K signal). The spectrum consists of two peaks separated by ca. 700 G on each side of a complex central signal, which itself is composed of several narrow lines and centered at $g \approx 2$. The seven components observed in the hyperfine structure of two identical nuclei of spin 3/2 are clearly visible. Together with a weak signal at the half-field value, these are characteristic of the existence of copper(II) ion pairs. The weak signal corresponds to the forbidden transition ($\Delta m_s = \pm 2$), whereas the signal observed at the normal magnetic field corresponds to the allowed transition ($\Delta m_s = \pm 1$).

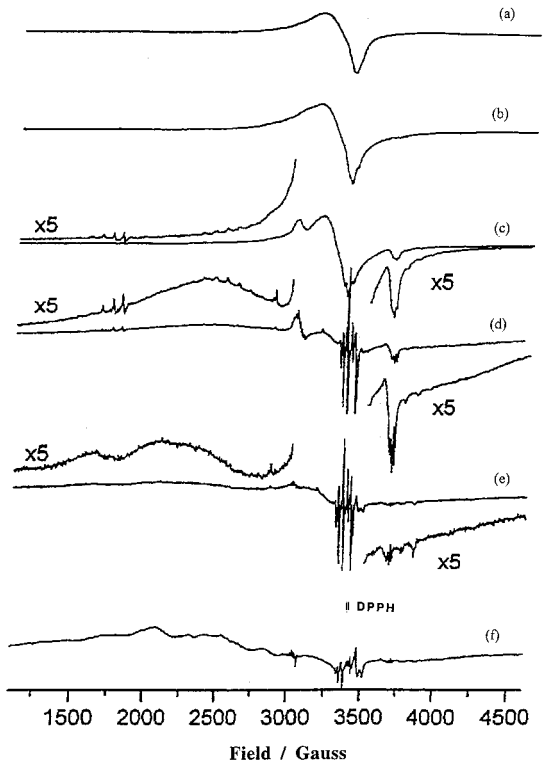

Figure 8. EPR spectra of the Cu(II)/CeO_2-imp (Cu:Ce = 0.1) catalyst material after drying at 333 K (a) and after calcination at 573 K (b), 873 K (c), 1073 K (d), 1173 K (e), and 1273 K (f).

Similar spectra are observed in Cu(II)/CeO_2-cop material with Cu:Ce atom ratio = 0.02 and Cu:Ce = 0.005. The formation of a Cu(II) ion dimer is still observable in the latter sample, though its presence is not so well defined after calcination at 873 K. Calcination of this low loading sample to 1273 K results in the appearance of a Ce^{3+} signal at $g = 1.959$.

In Situ Redox Reactions. The surface redox chemistry of the Cu/CeO_2 catalyst was investigated by an in situ examination of the Cu/CeO_2-cop (Cu:Ce = 0.01) material after calcination at 873 K. The corresponding material prepared by the impregnation route has a very similar constitution and behaves in a analogous fashion; hence, only the former is described here.

After calcination at 873 K, the catalyst comprises isolated Cu^{2+} ions, copper ion dimers, and amorphous aggregates adsorbed on the ceria particles, and the effect of exposure of the catalyst to CO is illustrated in Figure 9. Evacuation at 573 K has no effect on either the intensity or composition of the spectrum Figure 9b. Admission of 400 Torr CO to the sample at ambient temperature resulted in only a minor decrease in the intensity of the central signal together with a slight loss of resolution in the perpendicular component. A further loss of resolution occurred on heating the sample to 373 K still under 400 Torr CO. No further loss of intensity of either the central peak or dimer signals was observed. However, increasing the temperature to 473 K still under the CO atmosphere resulted in a significant change in the appearance of the spectrum. A marked

(15) Aboukais, A.; Bennain, A.; Aissi, Wrobel G, C. F.; Guelton, M.; Vedrine, M. *J. Chem. Soc., Faraday Trans.* **1992**, *88*, 615.
(16) Abi-Aad, E.; Bonnelle, J. P.; Aboukais, A. *J. Chem. Soc., Faraday Trans.* **1995**, *91*, 99.

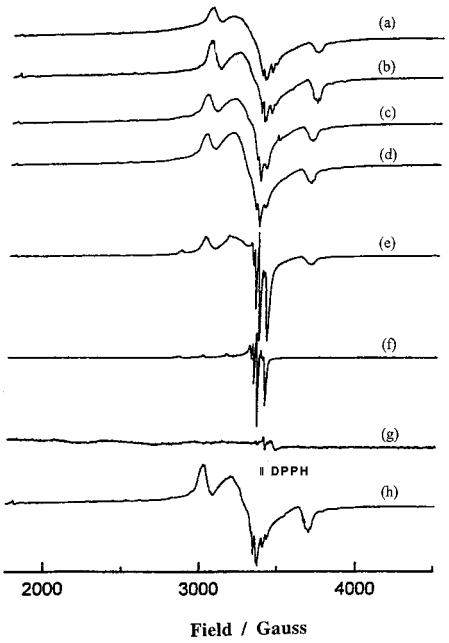

Figure 9. EPR spectra of the Cu(II)/CeO_2-cop (Cu:Ce = 0.01) catalyst material after calcination at 873 K (a) and after subsequent evacuation at 573 K and 10^{-2} Torr (b), followed by cooling to ambient temperature and exposure to CO (400 Torr) at ambient temperature (c), 373 K (d), 473 K (e), 573 K (f), and 673 K (g). (h) shows the spectrum following exposure of sample (g) to oxygen (400 Torr) at 673 K for 1 h.

increase in the resolution of the perpendicular region of the central signal is observed, mainly due to the removal of the broad isotropic signal attributed to amorphous CuO clusters. A further increase in temperature to 573 K resulted in the loss of the signal due to the dimer, leaving only the well-resolved peaks of monomeric Cu^{2+} ions. Thermal treatment at 673 K caused large scale reduction in the intensity of the remaining signal, and for the first time a resonance due to the presence of Ce^{3+} was noticeable. The original spectrum is restored completely on reoxidation of the sample by thermal treatment for 1 h at 673 K under an atmosphere of O_2 (400 Torr).

The reoxidation of the reduced catalyst material is more clearly seen in Figure 10. Exposure to 200 Torr O_2 at ambient temperature is sufficient to re-form both the isolated Cu^{2+} and dimeric Cu(II) ions. However, further increases in signal intensity are not observed at ambient temperature with increasing oxygen pressure, and heating to 373 K is required. Increasing the temperature to 473 K results in further reoxidation and the loss of resolution in the central peak, which can be attributed to the re-formation of Cu(II) aggregates with their inherent broad isotropic signal. Complete reoxidation is achieved after thermal treatment at 573 K under an atmosphere of oxygen.

Figure 11 shows the reoxidation of the reduced catalyst material by NO. The upper traces illustrate how the admission of NO at room temperature is enough to partially re-form isolated Cu^{2+} ions. However, thermal treatment at 323 K under 200 Torr NO is required to reform the Cu(II) ion dimers. Raising the temperature to 373 K significantly increases the intensity of all copper resonances, although resolution in the central peak is lost. This can again be attributed to the

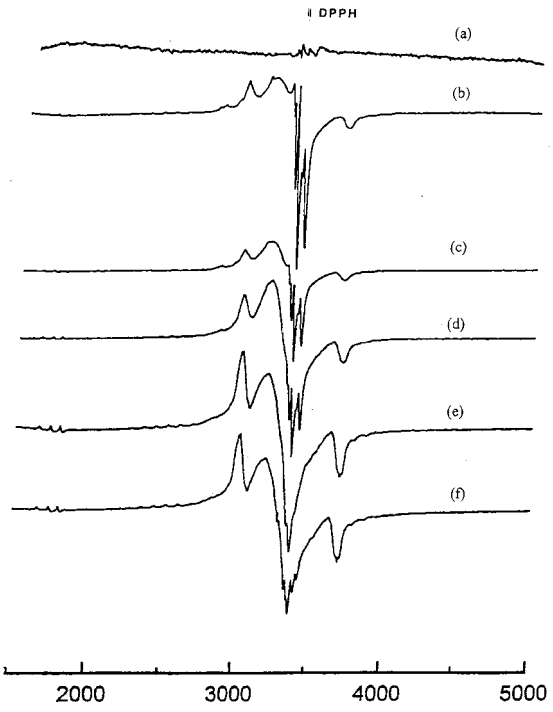

Figure 10. EPR spectra of the Cu(II)/CeO_2-cop (Cu:Ce = 0.01) catalyst material after calcination at 873 K and exposure to CO (400 Torr) at 673 K (a), followed by exposure to oxygen (200 Torr) at ambient temperature (b), 323 K (c), 373 K (d), 473 K (e), and 573 K (f).

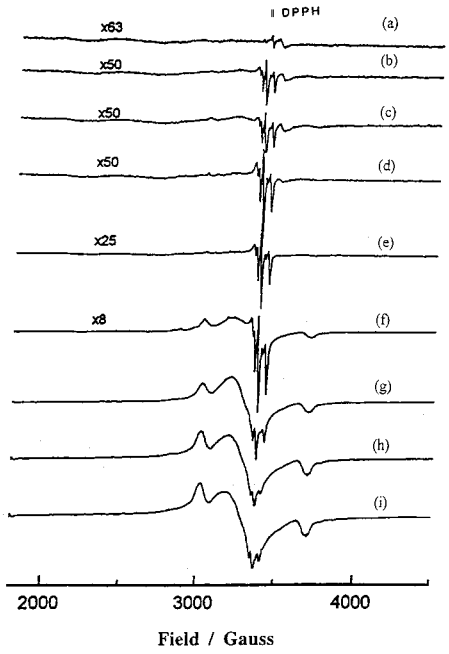

Figure 11. EPR spectra of the Cu(II)/CeO_2-cop (Cu:Ce = 0.01) catalyst material after calcination at 873 K and exposure to CO (400 torr) at 673 K (a), followed by exposure to NO at ambient temperature (2, 5, 20, and 200 Torr) (b−e), and exposure to NO (200 torr) at 323 K (f), 373 K (g), 473 K (h), and 573 K (i).

reformation of Cu(II) aggregates and the regeneration of the broad isotropic signal. This trend is continued on thermal treatment resulting in the complete reoxidation of the material by NO at 473 K.

Discussion

The oxidation of CO over promoted metal oxide catalysts is an area of catalysis which has been the center of discussion for many years, producing numerous and often conflicting models and mechanisms. The main areas of controversy include (i) the role of the metal promoter, (ii) the role of the metal oxide support, (iii) the interaction between promoter and support, (iv) the active sites for CO and O_2 adsorption, and (v) the mechanism. Both Rideal−Eley and Langmuir−Hinshelwood type reaction mechanisms have been proposed, but the former, in which adsorption of CO reacts with oxygen either activated on the oxide surface as superoxide ions (O_2^-) or extracted from the oxide lattice creating vacancies, appears to be preferred for promoted metal oxide catalysts such as ceria in light of its oxygen storage capacity.

Two parameters appear to exert a profound effect on the activity of promoted ceria catalyst materials toward the oxidation of carbon monoxide: (i) the thermal processing history; (ii) the nature and dispersion of the metal promoter. Unpromoted ceria effects the exhaustive oxidation of carbon monoxide when activated by precalcination at 673 K, although activity falls rapidly when calcination is carried out at temperatures ≥873K. Oxidation is achieved through adsorption of CO and abstraction of oxygen from the ceria lattice, creating lattice oxygen vacancies and the subsequent reduction of neighboring Ce^{4+} ions to Ce^{3+}. Adsorption of dioxygen regenerates the lattice oxygen sites and reoxidizing the metal ions to Ce^{4+}.

Promotion of ceria with copper(II) significantly reduces the temperature by which 100% conversion of carbon monoxide occurs, with the optimum activity observed for catalysts processed by thermal activation at 673 K. The level of copper(II) loading and the preparative methodology appeared to have a much lower effect on the catalytic activity. Precalcination at high temperatures (1273 K) or passing highly reducing gases (neat CO) over the catalyst leads to deactivation. Thermal deactivation is permanent and irreversible, but the latter type of deactivation can be reversed by heating the catalyst in a stream of air at 348 K.

A number of conclusions may be drawn from the catalytic actvity data. (1) The "active" catalyst results from thermal activation processing at ca. 673 K of the initial products obtained by a variety of preparative procedures. (2) Thermal processing at higher temperatures results in irreversible deactivation. (3) Reversible deactivation of the "active" catalyst occurs on exposure to reducing atmospheres. (4) The activity of the composite Cu(II)/CeO_2 catalyst toward the oxidation of carbon monoxide is greater than for either of the two individual oxides. These observations indicate the occurrence of both chemical and physical changes which affect the nature of the catalyst material.

We have employed two methods for the preparation of Cu(II)/CeO_2 catalyst materials: (i) coprecipitation from aqueous solutions containing Cu^{2+} and Ce^{4+} ions; (ii) sorption of Cu^{2+} ions on to preformed ceria gel. Coprecipitation is expected to produce a gel material in which copper(II) is incorporated into the cubic lattice of the microparticulate ceria. In contrast to analogous Cu(II)/SnO_2 catalyst materials, where both of these routes yield gel materials in which all copper(II) ions are present as surface species sorbed onto the tin(IV) oxide particulate, the nature of the copper species appears to be dependent on the preparative route for the copper-promoted ceria materials. As for the corresponding tin materials,[3] surface-sorbed hexaaqua $\{Cu(H_2O)_6\}^{2+}$ ions are formed from the sorption route. However, coprecipitation appears to produce a material in which the copper is present as (polymeric) $Cu(OH)_2$. presumably as a consequence of the much higher pH values needed in the case of ceria. It is also pertient to note that, in the case of ceria, neither method leads to the expected level of copper incorporation.

Thermal processing of these materials, which is important in their activation as CO oxidation catalysts, induces significant changes. The process by which particle growth occurs is by initial loss of physisorbed/hydrogen bonded molecular water, thereby exposing surface hydroxyl groups which can then condense forming interparticular "necks". Simultaneously two other processes occur at moderate calcination temperatures, the dehydration of the adsorbed hexaaqua $\{Cu(H_2O)_6\}^{2+}$ ions in the case of the Cu(II)/CeO_2-imp catalyst materials and a depolymerization of $Cu(OH)_2$ leading to well-dispersed copper(II) centers in the case of the Cu(II)/CeO_2-cop catalyst materials. These processes lead to similar materials from both preparative routes after treatment at 573 K comprising small (2.5 nm) particles of ceria which have a superficial amorphous oxide layer which has a disordered structure containing both cerium(IV) and copper(II) ions. At this stage no phase separation of CuO crystallites has yet occurred, and the copper(II) ions are dispersed in the superficial oxide layer and within ca. 4.2 Å of cerium(IV) ions. This composite material derived by calcination of the gel materials obtained initially by both routes exhibits the highest activity for carbon monoxide oxidation.

The surface concentration [M] of the promoter on the surface particles of a support oxide, assuming spherical, fully dense particles, is given by the expression

$$[\mathrm{M}] = \frac{\rho A d n \times 10^2}{6\mathrm{M}} \text{ atoms nm}^{-2} \qquad (1)$$

where ρ is the bulk density of the support oxide, A is Avogadro's number, d is the diameter of the support oxide particles (nm), M is the formula mass of the support oxide, and n is the fractional metal atom ratio of the promoter metal to support oxide. For copper-promoted ceria catalyst materials, this expression becomes

$$[\mathrm{Cu}] = 4.16(dn) \text{ atoms nm}^2 \qquad (2)$$

After thermal activation at 573 K the ceria particle size is 2.5 nm; hence for a Cu:Ce loading of 0.09 (the highest in this study), the surface [Cu] concentration on the surface of the ceria particles will be 0.94 Cu atoms nm^{-2}. Hence, at this loading the copper atoms are spaced apart by >1 nm in the thermally activated catalysts and can therefore be considered to be noninteracting. However, the EPR data shows that some loose clustering of the copper(II) centers is present for the material calcined at 573 K. The ceria crystallite size increases to 8.0 nm after calcination at 873 K, at which temperature some

phase separation of CuO is apparent by EXAFS. However, by 1273 K the material comprises relatively large crystals of CuO (63.5 nm) and ceria (85.0 nm). No significant incorporation of Cu(II) into the ceria lattice occurs.

EPR gives some insight into the nature of the copper species with calcination temperature. Spectra recorded for catalyst materials obtained by each preparative method are remarkably similar after the same thermal processing. After calcination at 573 K, the copper(II) is present in both types of material as a mixture of isolated Cu^{2+} ions and amorphous clusters or aggregates of Cu^{2+} ions. The same species are also present after calcination at 873 K, but additionally Cu^{2+} dimers are readily distiguished. Hence, the actual nature of the catalysts after calcination at these temperatures is much more complex than the EXAFS data would indicate.

In situ redox reactions using the $Cu(II)/CeO_2$-cop (0.09) catalyst material which has been precalcined at 873 K to produce a distribution of surface-dispersed copper(II) species show that all three types can be readily reduced by CO to (diamagnetic) Cu^{+}. The amorphous copper(II) dispersed on the ceria surface is reduced most easily at 473 K, followed by the dimer species at 573 K and finally the isolated Cu^{2+} monomers at 673 K when signals due to Ce^{3+} appear (i.e. reduction of the support). The relative resistance to reduction of the isolated copper(II) ions suggests that this type of copper(II) is located within growing crystallites of ceria, and hence, their accessibility to the gas phase is more limited compared with surface copper(II) species. Ce^{3+} species are only seen once near complete reduction of all copper species in the sample has been achieved, indicating that copper(II) is reduced in preference to cerium(IV) by CO.

Reoxidation of all types of Cu^{+} can be achieved by exposure of the reduced catalyst material to either O_2 or NO, although under the same pressure (200 Torr) oxidation by NO is achieved at a lower temperature than with O_2. The lack of $Cu^{+-}NO$ signals in the EPR spectra, as observed by Giamello et al.[17] and Aylor et al.,[18] indicates that NO does not bind to Cu sites but rather to the ceria surface. Studies by Soria et al.[19,20] have shown that the presence of oxygen vacancies at the ceria surface promote the decomposition (and hence reduction) of NO. Hence, the order of reduction of the Cu species is amorphous aggregates > dimers > monomers, while reoxidation follows the opposite order.

Mechanism of Reaction. The active catalyst is produced by thermal processing of $Cu(II)/CeO_2$ materials obtained either by coprecipitation or impregnation methods at 673 K and comprises particles of ceria which have a superficial disordered amorphous oxide layer containing both cerium(IV) and copper(II) ions.

It is open to speculation what role copper(II) plays in catalysts which have been thermally activated. Synergism between the two components has been proposed to be the origin of the high activity in mixed Fe_2O_3/SnO_2,[21] Mn_2O_3/SnO_2,[21] and Cu/SnO_2[3,22] catalysts. Both $Cu(II)/SnO_2$[3] and $Cu(II)/CeO_2$[4,23] catalysts function efficently for CO oxidation at very low temperatures, where no significant copper reduction occurs as previously observed for both unsupported copper(II) oxide[24] and other supported copper(II) catalysts such as $Cu(II)/Al_2O_3$.[25−27] Hence, it may be concluded that both components are important for the high catalytic activity observed in the present case, which raises the question of how the synergism operates.

Like the analogous $Cu(II)/SnO_2$ catalyst materials, the mode of action of the $Cu(II)/CeO_2$ catalysts appears to be via the reduction of a surface copper(II) by CO by the abstraction of a surface oxygen by gas phase CO forming carbon dioxide which desorbs leaving a surface vacancy together with a negative charge. The role of the copper(II) is to scavenge the negative charge and be reduced to copper(I). Dissociative chemisorption of dioxygen or nitrogen oxides replenishes the surface vacancies and reoxidizes copper(I) to copper(II). The intermediate formation of nitrous oxide in the CO/NO reaction is most probably due to the reaction of NO molecules with adsorbed nitrogen atoms.

The catalyst can be deactivated reversibly by exposure to highly reducing atmospheres such as high concentrations of carbon monoxide or irreversibly by thermal treatment at very high temperatures. Reversible deactivation occurs by the depletion of surface oxygen by abstraction by CO, but this may be restored by treatment with molecular oxygen. The irreversible deactivation can be attributed to two processes which occur at temperatures ≥873 K, the phase separation of copper(II) oxide particles and rapid particle size growth which severely reduces the specific surface area. The onset of rapid particle size growth occurs at temperatures ≈873 K. Crystalline copper(II) oxide is observed after processing at 1273 K and is observed by EXAFS after processing at 873 K.

Thus the major factor affecting nature of the $Cu(II)/CeO_2$ catalyst materials is the temperature of the pretreatment activation processing. The preparative route and the level of copper loading are less important. A summary relating the CO activity properties and catalyst deactivation with the constitution of the materials at various processing temperatures is shown in Table 6.

Conclusions

$Cu(II)/CeO_2$ catalyst materials can be prepared by two either coprecipitation from aqueous solutions containing Cu^{2+} and Ce^{4+} ions or by sorption of Cu^{2+} ions on to preformed ceria gel.

The coprecipitation and impregnation routes give materials comprising polymeric $Cu(OH)_2$ and hexaaqua $\{Cu(H_2O)_6\}^{2+}$ ions, respectively, sorbed onto ceria particles.

(17) Giamello, E.; Murphy, D.; Anpo, M. *J. Catal.* **1992**, *136*, 510.
(18) Aylor, A.; Larsen, S.; Bell, A. T. *J. Catal.* **1995**, *157*, 592.
(19) Soria, J.; Martinez-Arias, A.; Conesa, J. C. *J. Chem. Soc., Faraday Trans.* **1995**, *91*, 1669.
(20) Martinez-Arias, A.; Soria, J.; Cataluna, R. *J. Chem. Soc., Faraday Trans.* **1995**, *91*, 1679.
(21) Kulshreshtha, S. K.; Gadgil, M. M.; Sasikaia, R. *Catal. Lett.* **1996**, *37*, 181.
(22) Martinez-Arias, A.; Fernandez-Garcia, M.; Soria, J.; Conesa, J. C. *J. Catal.* **1999**, *182*, 367.
(23) Daniell, W. Ph.D. Thesis, University of Nottingham, 1998.
(24) Jernigan G. G.; Somorjai, G. A. *J. Catal.* **1994**, *147*, 567.
(25) Severino, F.; Brito, J.; Carias, O.; Laine, J. *J. Catal.* **1986**, *102*, 172.
(26) Choi, K. I.; Vannice, M. A. *J. Catal.* **1991**, *131*, 22.
(27) Park, P. W.; Ledford, J. S. *Appl. Catal. B* **1998**, *15*, 221.

Table 6. Summary of the Nature of Cu(II)/CeO$_2$ Catalyst Materials after Various Pretreatment Temperatures

pretreatment temp (K)	nature of catalyst mater	activity toward CO oxidn	comments
333	*by impregation*, Cu present largely as $\{Cu(H_2O)_6\}^{2+}$ ions adsorbed on the surf of tin(IV) oxide nanocystallites; *by coprecipitation*, Cu present largely as polymeric $Cu(OH)_2$ adsorbed on the surf of cerium(IV) oxide nanocystallites	exhibits greater activity than either CuO or CeO$_2$ alone but not as high as after thermal processing at 573 K	
573−673	comprises small CeO$_2$ particles with a superficial amorphous oxide layer which has a disordered structure containing both cerium(IV) and copper(II) ions; no phase separation of CuO crystallites has yet occurred, and the copper(II) ions are dispersed in an amorphous superficial oxide layer	exhibits the highest activity for CO oxidation, with light-off at ca. 300 K and complete conversion at ca. 355K; once initiated the reacn is self-sustaining	catal is deactivated by running under highly reducing conditions, but activity is restored by thermal processing in a stream of air at 348 K
873	onset of rapid particle size growth; CuO is observed by EXAFS	complete CO conversion not achieved until 487 K, but activity still better than either CuO or CeO$_2$ alone	
1273	CeO$_2$ particle size 85 nm; crystalline CuO (particle size 63.5 nm) obsd	activity poor with light-off temp similar to that of CuO; complete conversion not achieved until ca. 727 K	loss of activity irreversible

The most active catalyst material is formed by thermal processing of materials obtained by either route at ca. 673 K producing a material comprising small particles of ceria on the surface of which copper(II) is dispersed amorphously.

In catalysts calcined at high temperatures (1273 K), the copper is segregated as copper(II) oxide crystallites and the particles of ceria are very large (ca. 85 nm). These materials are relatively inactive.

Promotion of ceria with copper(II) enhances the activity toward the oxidation of carbon monoxide dramatically. A 100% conversion occurs at 343 K even for high CO concentrations and stoichiometric CO/O$_2$ compositions.

Only surface copper(II) is reactive in a catalytic sense with CO, since bulk copper(II) only reacts with CO under relatively extreme conditions. At ambient temperature surface copper(II) species are reduced quite slowly to copper(I) on exposure to CO, but facile reduction of surface copper(II) occurs on heating to ≈373 K.

EPR shows that, after calcination at 573 K, the copper(II) is present in both types of material as a mixture of isolated Cu^{2+} ions and amorphous clusters or aggregates of Cu^{2+} ions. The same species are also present after calcination at 873 K, but additionally Cu^{2+} dimers are present.

In situ redox studies show that the amorphous copper(II) aggregates are reduced most easily by exposure to CO at 473 K, followed by the dimer species at 573 K and finally the isolated Cu^{2+} monomers at 673 K when signals due to Ce^{3+} appear (i.e. reduction of the support). Reoxidation of all types of Cu^{+} can be achieved by exposure of the reduced catalyst material to either O_2 or NO, although under the same pressure (200 Torr) oxidation by NO is achieved at a lower temperature than with O_2.

The mode of action of these catalyst materials appears to be via the abstraction of a surface oxygen by CO followed by desorption of CO_2. The role of copper(II) is to scavenge the negative charge formed when CO abstracts surface oxygen and is thereby reduced to copper(I). Dissociative chemisorption of dioxygen or a nitrogen oxide replenishes the surface vacancies and reoxidizes copper(I) to copper(II). The significant enhancement of catalytic activity is due in large part to the efficiency of the Cu(II)/Cu(I) couple in this process.

Catalyst deactivation at low temperatures under reducing conditions is due to depletion of the catalyst surface of active oxygen. The catalytic activity is restored by treatment in air at moderate temperatures. Deactivation at high temperatures is irreversible and is due to the phase separation of copper(II) oxide coupled with a dramatic increase in particle size.

Acknowledgment. We thank the Commission of the European Community (Contract No. AVI* CT92-0012) and the EPSRC (for Research Grant No. GR/J76026 and providing facilities at DRAL) for support and the Malaysian Government (for the award of a scholarship to W.A.).

CM001113K